

Coupled Fluid Flow and Thermal and Reactive Transport in Porous Media for Simulating Waste Stabilization Phenomena in Semi-aerobic Landfill

H. Ishimori^{*1}, K. Endo¹, T. Ishigaki¹, H. Sakanakura¹, and M. Yamada¹

¹ National Institute for Environmental Studies, Japan

* Corresponding author:

16-2, Onogawa, Tsukuba, Ibaraki, 305-8506, Japan, ishimori.hiroyuki@nies.go.jp

Abstract: Semi-aerobic landfill has interesting structure that passively provides the atmospheric oxygen into landfilled waste due to the heat convection generated by the decomposition of landfilled waste. There are limited studies on the mechanisms of the oxygen transport. That is, what driving force transports oxygen into the landfilled waste layer? and how much oxygen is transported into the landfilled waste layer? In order to solve these problems quantitatively, it is necessary to formulate the governing equation systems for gas fluid flow and thermal and reactive transport in the landfill. COMSOL Multiphysics was useful for modeling such complex equation systems and solving them. This paper presents the governing equations and parameter estimation methods for the numerical simulation of the gas fluid flow and thermal and reactive transport in landfill. Finally, it shows the results of the numerical simulations for semi-aerobic landfill and anaerobic landfill.

Keywords: Density-dependent gas flow, Multi-component gas transport, Parameter estimation, Multiphysics analysis

1. Introduction

Landfill gases such as methane and carbon dioxide which are generated from biological waste decomposition in the waste stabilization process, have an environmental impact on global warming. The structure of semi-aerobic landfill as shown in Fig. 1 has been considered effective for enhancing the waste stabilization as well as reducing the global warming impact. The semi-aerobic landfill has vertical gas extraction wells and horizontal drainage wells. When their wells are jointed, the atmospheric air in the drainage wells are warmed by heat generated from the biological waste decomposition reactions, and the warmed air can be naturally provided to

waste layer because of the lowered gas density and the buoyant force. Oxygen in the air can work for enhancing the waste decomposition reactions and reducing the methane which has a large global warming potential. In addition, the other gases including carbon dioxide generated from the reactions can be transported to the gas extraction wells and they are treated as needed. The theoretical mechanism of semi-aerobic landfill has been of a great concern to investigate its performance.

COMSOL Multiphysics ver 3.5a was used to clarify the gas transport phenomena in semi-aerobic landfill. Numerical model consisted of (1) mixture-gas flow equation based on Darcy's law, (2) multicomponent gas transport equations based on Fickian diffusion law, and (3) heat transfer equation. The multicomponent gas was methane, carbon dioxide, oxygen, and nitrogen. These equation systems were formalized using Earth Science Module and Chemical Engineering Module. In addition, their mobility parameters such as gas density, dynamic viscosity, diffusion coefficient, specific heat capacity, and heat conductivity were theoretically estimated using Chemical Reaction Engineering Lab.

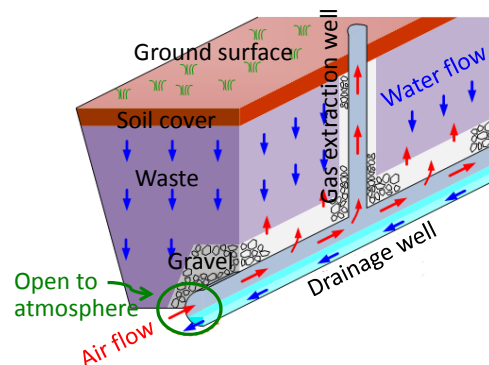


Fig. 1: Structure of semi-aerobic landfill

2. Governing Equations

2.1 Gas flow equation

When the landfilled waste layer is assumed isotropic porous media, the volumetric velocity of the gas fluid flow is given by Darcy's law:

$$\mathbf{u}_g = -\frac{K}{\eta_g} (\nabla p_g + \rho_g g \nabla z) \quad (1)$$

where, \mathbf{u}_g = volumetric gas velocity (m/s), K = intrinsic permeability (m^2), η_g = gas viscosity (Pa s), p_g = gas pressure (Pa), ρ_g = gas density (kg/m^3), g = gravity acceleration ($= 9.82 \text{ m}/\text{s}^2$). It is noted that fully-dry condition was assumed in this study. Governing equation is as follows:

$$\phi \frac{\partial \rho_g}{\partial t} + \nabla \cdot \left[-\rho_g \frac{K}{\eta_g} (\nabla p_g + \rho_g g \nabla z) \right] = \sum_i R_i \quad (2)$$

here, ϕ = porosity, R_i = source/sink term for gas component i , i = gas index for CH_4 , CO_2 , O_2 , or N_2 .

2.2 Gas transport equations

Transport equations are used for calculating the concentration of each gas component. Since various gas components are included in landfill, the gas fraction is diluted by the concentration of each other. Transport of diluted gas components is formulated as:

$$\phi \frac{\partial c_i}{\partial t} + \nabla \cdot (-\phi \tau D_{ig} \nabla c_i + \mathbf{u}_g c_i) = \frac{R_i}{M_i} \quad (3)$$

here, c_i = molar concentration of gas component i (mol/m^3), τ = tortuosity, M_i = molecular weight of gas component i (mol/kg), and D_{ig} = diffusion coefficient of gas component i (m^2/s).

The molar fraction and the mass fraction are calculated as follows:

$$\chi_i = \frac{c_i}{\sum_j c_j} \quad (4)$$

$$\omega_i = \frac{\chi_i M_i}{\sum_j \chi_j M_j} \quad (5)$$

here, χ_i = molar fraction of gas component i , and ω_i = mass fraction of gas component i .

(1) Methane generation

Methane is generated under fully anaerobic condition. On calculation, however, the methane can be allowed to be generated even in a certain

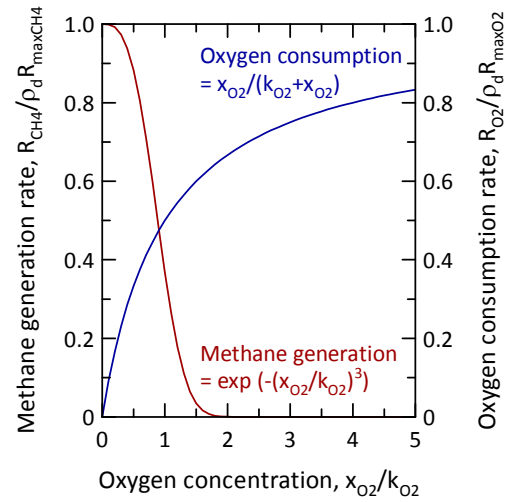


Fig. 2: Source/sink functions for methane and oxygen

representative elementary volume that has some oxygen concentration, not fully anaerobic. It is because the methane gas is apparently generated from the representative elementary volume when the elementary volume has both a fully anaerobic area and an aerobic area with some oxygen in microscale. The methane generation rate, R_{CH_4} , was assumed formulated as follows:

$$R_{\text{CH}_4} = \rho_d R_{\text{maxCH}_4} \exp\left(-\left(\frac{\chi_{\text{O}_2}}{k_{\text{O}_2}}\right)^3\right) \quad (6)$$

where, R_{CH_4} = methane generation rate from landfilled waste layer ($\text{kg}/\text{m}^3/\text{s}$), R_{maxCH_4} = the maximum methane generation rate ($1/\text{s}$), ρ_d = bulk dry density of the landfilled waste layer (kg/m^3), χ_{O_2} = molar fraction of oxygen, and k_{O_2} = threshold value for oxygen concentration when methane is generated from the landfilled waste layer. Equation (6) expresses that the methane generates in the oxygen molar fraction of $< k_{\text{O}_2}$ as shown in Fig. 2.

(2) Carbon dioxide dissolution

The pore water in the waste layer where incinerated ashes are landfilled has a high pH value. In this case, the carbon dioxide that is generated from the waste layer or is transported from the atmosphere can dissolve into the pore water. The carbon dioxide dissolution rate, R_{CO_2} , was assumed formulated as follows:

$$R_{\text{CO}_2} = -\phi \lambda_{\text{CO}_2} M_{\text{CO}_2} c_{\text{CO}_2} \quad (7)$$

where, R_{CO_2} = carbon dioxide dissolution rate in landfilled waste layer ($kg/m^3/s$), and λ_{CO_2} = first order dissolution rate for the carbon dioxide (1/s). Essentially, the source/sink term must include the carbon dioxide generation from the landfilled waste layer. However, the carbon dioxide has been considered to rapidly dissolve into the pore water with a high pH value. Thus, the generation of the carbon dioxide from the waste layer was not considered in this study.

(3) Oxygen consumption

Oxygen in landfilled waste layer is used for the biological waste decomposition reactions. The oxygen consumption, R_{O_2} , is given as

$$R_{O_2} = -\rho_d R_{maxO_2} \frac{S}{k_s + S} \frac{\chi_{O_2}}{k_{O_2} + \chi_{O_2}} \quad (8)$$

R_{O_2} = oxygen consumption rate in landfilled waste layer ($kg/m^3/s$), R_{maxO_2} = the maximum oxygen consumption rate (1/s), S = available substrate as equivalent oxygen consumption, and k_s = substrate half-saturation constant. Figure 2 shows the function of Eq. (8) when the substrate, S , is enough.

2.3 Heat transfer equation

Heat generates when the landfilled waste is biologically decomposed. The temperature in the landfilled waste layer is generally higher than that in atmosphere. This temperature gradient from the waste layer to the atmosphere becomes the driving force to passively transport the gas components such as methane, carbon dioxide, oxygen, and nitrogen. Heat transfer equation is represented as

$$C_{eq} \frac{\partial T}{\partial t} + \nabla \cdot (-\lambda_{eq} \nabla T + C_{eq} u_g T) = Q_T \quad (9)$$

T = absolute temperature (K), λ_{eq} = equivalent heat conductivity (W/m/K), C_{eq} = equivalent heat capacity ($J/m^3/K$), and Q_T = heat generation rate from landfilled waste layer ($J/m^3/s$).

The equivalent heat conductivity is given as

$$\lambda_{eq} = \phi \lambda_g + (1 - \phi) \lambda_s \quad (10)$$

where, λ_s = heat conductivity of solid phase (W/m/K), and λ_g = heat conductivity of gas phase (W/m/K). In addition, the equivalent heat capacity is given as

$$C_{eq} = \phi \rho_g c_{pg} + \rho_d c_{ps} \quad (11)$$

where, c_{ps} = specific heat capacity of solid phase (J/kg/K), and c_{pg} = specific heat capacity of gas phase. It is noted that Eqs. (10) and (11) were assumed fully dry condition.

The heat generation rate from the landfilled waste layer was assumed given as

$$Q_T = \alpha (T_{wst} - T) \quad (12)$$

α = heat generation constant ($W/m^3/K$), and T_{wst} = equilibrium temperature in the landfilled waste layer (K). The observed temperature in landfill was used for the equilibrium temperature.

3. Parameter Estimations

3.1 Gas density

Gas density is dependent on the gas pressure, concentrations, and temperature. Gas ideal law is represented as

$$\rho_g = \frac{P_g}{R_g T} \sum_i \chi_i M_i \quad (13)$$

where, R_g = gas constant (= 8.314 J/mol/K).

3.2 Gas viscosity

Gas viscosity is given as a function of the gas concentrations and temperature. There are well-known estimation methods such as Sutherland's empirical equation and Chapman-Enskog theory. Their methods have been considered to estimate the gas viscosity with extremely good accuracy. According to Sutherland's empirical equation, the viscosity of pure gas which consists of only one component is given as

$$\eta_i = \eta_{i0} \left(\frac{T_0 + C_i}{T + C_i} \right) \left(\frac{T}{T_0} \right)^{3/2} \quad (14)$$

T_0 = reference temperature (K), η_i = viscosity of gas component i (Pa s), η_{i0} = reference viscosity of gas component i at reference temperature (Pa s), C_i = Sutherland's constant of gas component i . Table 1 summarizes the reference viscosity and the Sutherland's constant of methane, carbon dioxide, oxygen, and nitrogen.

Gas viscosity is estimated by the viscosities and the concentrations of the gas components. Wilke's equation is defined as:

$$\eta_g = \sum_i \frac{\eta_i \chi_i}{\sum_j \phi_j \chi_j} \quad (15)$$

Table 1: Parameters for estimating viscosity and diffusion coefficient

| | Chemical formula | Molecular weight, M (x10 ⁻³ kg/mol) | Viscosity at 25°C, η (x10 ⁻⁵ Pa s) | Sutherland's constant, C (K) | Collision diameter, σ (10 ⁻¹⁰ m) | Characteristic energy, ε/k _b (T) |
|----------------|------------------|--|---|------------------------------|---|---|
| Methane | CH ₄ | 16 | 1.10 | 164 | 3.758 | 148.6 |
| Carbon dioxide | CO ₂ | 44 | 1.47 | 240 | 3.941 | 195.2 |
| Oxygen | O ₂ | 32 | 2.04 | 125 | 3.467 | 106.7 |
| Nitrogen | N ₂ | 28 | 1.76 | 104 | 3.798 | 71.4 |

where,

$$\phi_{ij} = \frac{\left[1 + (\eta_i/\eta_j)^{1/2} (M_j/M_i)^{1/4}\right]^2}{\left[8(1 + M_i/M_j)\right]^{1/2}} \quad (16)$$

Namely, summarized procedure is as follows: the viscosities of gas component *i* at a temperature were first estimated according to Sutherland's equation, and then the viscosity of mixture gas which consists of their component was estimated using Wilke's equation.

3.3 Gas diffusion coefficient

Diffusion coefficient of gas component *i* into mixture gas can be evaluated by binary diffusion coefficient and concentration of each component. The binary diffusion coefficient of component *i* to *j* is estimated from Chapman-Enskog theory as follows.

$$D_{ij} = \frac{5.953 \times 10^{-4}}{P_g \sigma_{ij} \Omega_D} \sqrt{\frac{T^3}{M_i} + \frac{T^3}{M_j}} \quad (17)$$

here, D_{ij} = binary diffusion coefficient (m²/s), σ_{ij} = average collision diameter of gas component *i* and *j* (10⁻¹⁰ m), and Ω_D = collision integral. The collision integral is given as

$$\Omega_D = \frac{1.060}{T_N^{0.156}} + \frac{0.193}{e^{0.476T_N}} + \frac{1.036}{e^{1.530T_N}} + \frac{1.765}{e^{3.894T_N}} \quad (18)$$

where,

$$T_N = \frac{T}{\sqrt{\varepsilon_i/k_b} \sqrt{\varepsilon_j/k_b}} \quad (19)$$

T_N = standardized temperature, ε = characteristic energy (J), and k_b = Boltzman's constant (= 1.38 x 10⁻²³ J/K). Parameters for estimation of binary

diffusion coefficients in methane, carbon dioxide, oxygen, and nitrogen are also listed in Table 1.

Fickian diffusion coefficient can be estimated using the binary diffusion coefficients and the concentrations of the gas components include the mixture gas as follows.

$$D_{ig} = \frac{1 - \chi_i}{\sum_{j:j \neq i} \frac{\chi_j}{D_{ij}}} \quad (20)$$

here, D_{ig} = Fickian diffusion coefficient of gas component *i* into the mixture gas (m²/s), and it was used for the Fickian diffusion equations as shown in Eq. (3).

3.4 Gas heat conductivity

Although gas heat conductivity can be also estimated from the Chapman-Enskog theory, the estimation for the heat conductivity has been considered not accurate compared with that for the viscosity. In this study, therefore, the heat conductivity of gas component *i* was estimated using parameters in thermodynamic database,

$$\lambda_i = \frac{C_1 T^{C_2}}{1 + C_3/T + C_4/T^2} \quad (21)$$

where, λ_i = heat conductivity of gas component *i* (W/m/K), and C_i = model parameters obtained from general DIPPR and JANAF databases. The used parameters are summarized in Table 2.

Gas heat conductivity was estimated from the heat conductivities and concentrations of gas components as follows.

$$\lambda_g = \frac{1}{2} \left(\sum_i \lambda_i \chi_i + \left(\sum_i \frac{\chi_i}{\lambda_i} \right)^{-1} \right) \quad (22)$$

Table 2: Parameters for estimating heat conductivity

| $\lambda_i = \frac{C_1 T^{C_2}}{1 + C_3/T + C_4/T^2}$ | | | | | | |
|---|------------------|--|-------------------------------------|----------------|---|------------------------------------|
| | Chemical formula | Molecular weight, M (x10 ⁻³ kg/mol) | C ₁ (x10 ⁻⁴) | C ₂ | C ₃ ² (x10 ²) | C ₄ (x10 ⁶) |
| Methane | CH ₄ | 16 | 0.0840 | 1.4268 | -0.49654 | 0 |
| Carbon dioxide | CO ₂ | 44 | 36,900 | -0.3838 | 9.64000 | 1.8600 |
| Oxygen | O ₂ | 32 | 4.4994 | 0.7456 | 0.56699 | 0 |
| Nitrogen | N ₂ | 28 | 3.3143 | 0.7722 | 0.16323 | 0.0004 |

Table 3: Parameters for estimating specific heat capacity

| $c_{pi} = \frac{10^{-3}}{M_i} \left(C_1 + C_2 \left[\frac{C_3/T}{\sinh(C_3/T)} \right]^2 + C_4 \left[\frac{C_5/T}{\cosh(C_5/T)} \right]^2 \right)$ | | | | | | | |
|---|------------------|--|------------------------------------|------------------------------------|---|------------------------------------|----------------|
| | Chemical formula | Molecular weight, M (x10 ⁻³ kg/mol) | C ₁ (x10 ⁵) | C ₂ (x10 ⁵) | C ₃ ³ (x10 ³) | C ₄ (x10 ⁵) | C ₅ |
| Methane | CH ₄ | 16 | 0.33298 | 0.79933 | 2.0869 | 0.41602 | 992.0 |
| Carbon dioxide | CO ₂ | 44 | 0.29370 | 0.34540 | 1.4280 | 0.26400 | 588.0 |
| Oxygen | O ₂ | 32 | 0.29103 | 0.10040 | 2.5265 | 0.09356 | 1153.8 |
| Nitrogen | N ₂ | 28 | 0.29105 | 0.08615 | 1.7016 | 0.00103 | 909.8 |

3.5 Gas specific heat capacity

Specific heat capacity of gas component *i* can be also estimated using the DIPPR and JANAF thermodynamic databases.

$$c_{pi} = \frac{10^{-3}}{M_i} \left(C_1 + C_2 \left[\frac{C_3/T}{\sinh(C_3/T)} \right]^2 + C_4 \left[\frac{C_5/T}{\cosh(C_5/T)} \right]^2 \right) \quad (23)$$

c_{pi} = specific heat capacity of gas component *i* (J/kg/K), and C_i = model parameters obtained from the DIPPR and JANAF databases. Table 2 summarizes the parameters used in this study.

Gas specific heat capacity is given as

$$c_{pg} = \sum_i \omega_i c_{pi} \quad (24)$$

where, c_{pg} = gas specific heat capacity (J/kg/K).

4. Use of COMOSL Multiphysics

4.1 Objective

Objective of the numerical gas flow and transport simulation for semi-aerobic landfill was to clarify (1) whether oxygen in atmosphere is provided into the landfilled waste layer due to the heat convection, and (2) how much oxygen is transported into the landfilled waste layer.

4.2 Analysis domains

The simplified analysis domain in the cross-sectional two dimension for semi-aerobic landfill is shown in Fig. 3(a). In contrast, the structure of the anaerobic landfill is shown in Fig. 3(b) as control. These domains were 6 m long in the *x*-direction and 4.5 m deep in the *y*-direction, and consisted of two layers (one was the landfilled waste layer with thickness of 4 m and the other was the soil cover layer with thickness of 0.5 m). The drainage well with the diameter of 400 mm was installed in the bottom of the domain, and the gravel layer was installed around the well. In

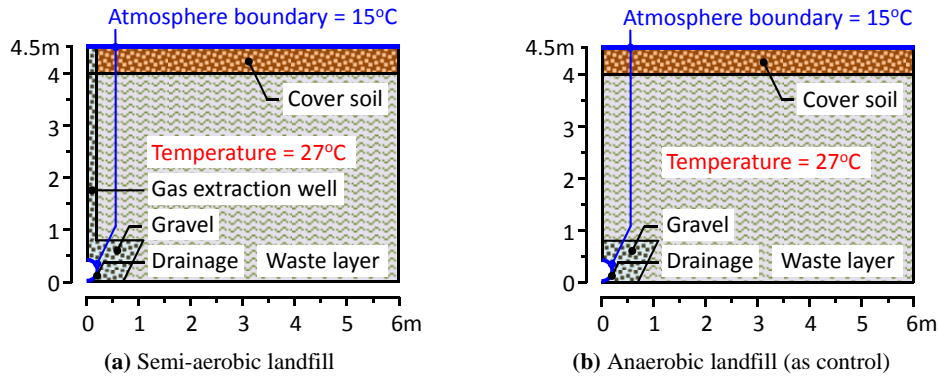


Fig. 3: Analysis domain

Table 4: Analysis condition

| Parameter | Unit | Waste layer | Cover soil | Gravel |
|--|---------------------|-------------------|-------------------|-------------------|
| Porosity (ϕ) | | 0.30 | 0.30 | 0.50 |
| Bulk dry density (ρ_d) | kg/m ³ | 1,200 | 1,800 | 1,500 |
| Intrinsic permeability (K) | m ² | 10 ⁻¹² | 10 ⁻¹⁴ | 10 ⁻¹⁰ |
| Tortuosity (τ) | | 0.67 | 0.67 | 0.79 |
| Max. CH ₄ generation rate ($R_{\max\text{CH}_4}$) | mg/g/d | 10 ⁻² | 0 | 0 |
| Max. O ₂ consumption rate ($R_{\max\text{O}_2}$) | mg/g/d | 10 ⁻¹ | 0 | 0 |
| Specific heat capacity (c_{ps}) | J/m ³ /K | 1,000 | 800 | 1,200 |
| Heat conductivity (λ_s) | J/kg/K | 0.95 | 0.40 | 0.40 |

addition, the semi-aerobic landfill as shown in Fig. 3(a) had the gas extraction well with the diameter of 400 mm and the well was jointed to the drainage well.

4.3 Analysis conditions

Table 4 summarizes the analysis conditions. For the settings of material properties, the cover soil was assumed general decomposed granite soil, and the landfilled waste was assumed an incinerated ash. Gas properties such as density, viscosity, diffusion coefficient, heat conductivity, and specific heat capacity were determined using estimation methods described in previous section.

4.4 Results

Figures 4 and 5 are the stationary distribution of the gas pressure, the oxygen concentration, and the temperature in semi-aerobic landfill and landfill without gas extraction wells, respectively. In the semi-aerobic landfill, the atmospheric air

around the drainage well was warmed and its gas density was lowered so that it naturally moved up according to the buoyant force. The oxygen in the air around the gas extraction well diffused into waste layer. The oxygen diffused into the waste layer was used for waste decomposition reactions and was expected to enhance the waste stabilization. However, in the landfill without the gas extraction well, the air could not move up even if the buoyant force was generated because the gas permeability of the waste layer was smaller than that of the gravel. Thus, the oxygen hardly diffused into the waste layer.

Figure 6 shows the difference in the oxygen inflow rate from the drainage well in the semi-aerobic landfill and the landfill without the gas extraction wells. The structure of the semi-aerobic landfill can passively provide the oxygen that requires for biological waste decomposition reactions into waste layer in any cases tested.

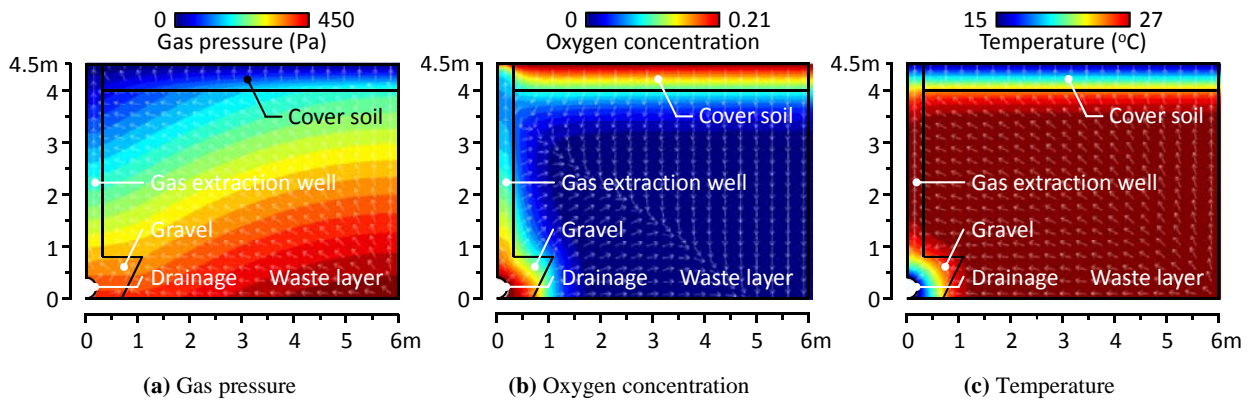


Fig. 4: Results for semi-aerobic landfill

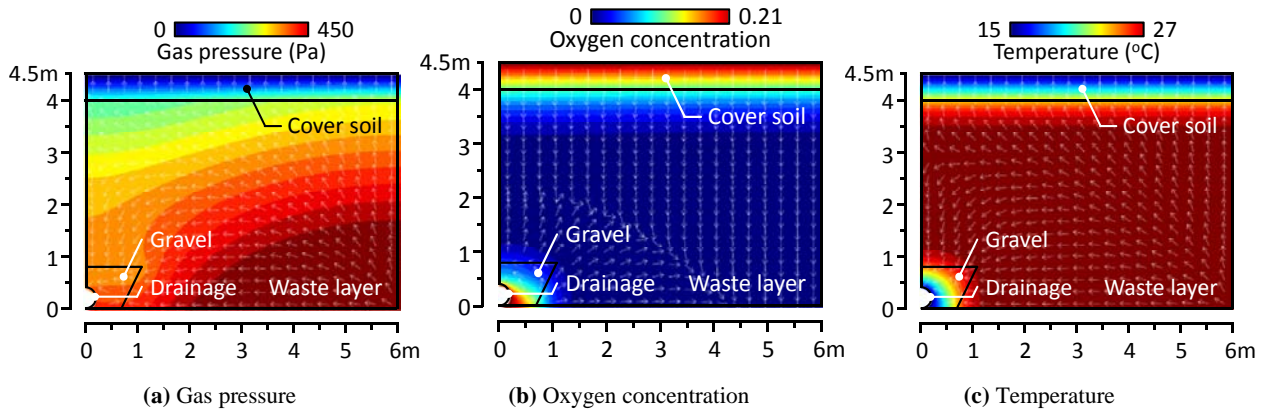


Fig. 5: Results for landfill without gas extraction well (anaerobic landfill)

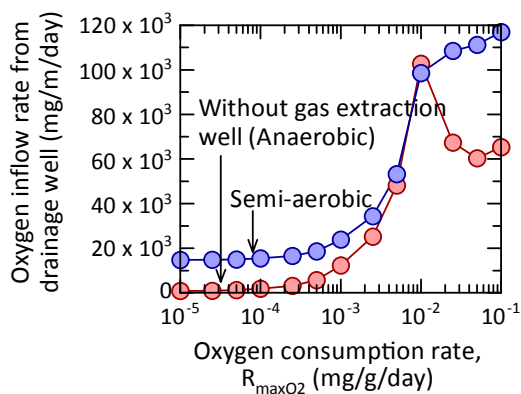


Fig. 6: Results of calculated oxygen inflow rate from drainage well into landfill

5. Conclusions

COMSOL Multiphysics was useful to clarify such a complex migration and transport of gas in semi-aerobic landfill. It was concluded that the structure of semi-aerobic landfill can passively provide the oxygen, which requires for biological waste decomposition reactions, into waste layer. The numerical model used in this study will be available for the landfill structure optimization to make the oxygen inflow rate into the landfill maximized.

Such a complex numerical analysis requires a lot of computational complexity. Although this study discussed under limited analysis conditions in two dimensional and stationary analysis, a further discussion will be advanced using the technique of a gpgpu and a parallel computing.